

Expression and potential regulation of miRNA-431 during lung development of Sprague-Dawley rats

ZHONG-YI SUN¹, YAN-QING SHEN², XIAO-QING CHEN¹, XIAO-YU ZHOU²,
RUI CHENG², ZHI-DAN BAO³ and YANG YANG²

¹Department of Pediatrics, The First Affiliated Hospital, Nanjing Medical University, Nanjing, Jiangsu 210029;

²Department of Neonates, Children's Hospital of Nanjing Medical University, Nanjing, Jiangsu 210008;

³Department of Neonates, Jiangyin People's Hospital of Nanjing Medical University, Wuxi, Jiangsu 210008, P.R. China

Received September 28, 2018; Accepted March 27, 2019

DOI: 10.3892/mmr.2019.10154

Abstract. Deficiency of surfactant proteins (SPs) is the main cause of respiratory distress syndrome (RDS) and chronic lung diseases. Our previous study demonstrated that miR-431 was differentially expressed between infants with RDS and infants without RDS using microarray analysis. However, the potential role of miR-431 in the development of lung function is still unknown. In the present study, the morphological characteristics of lung tissues and the expression levels of miR-431 were examined at three time points of rat lung development [gestational days 19 and 21 (E19, and E21) and postnatal day (P3)]. The protein and mRNA levels of SMAD4 and SPs (SP-A, SP-B, SP-C and SP-D) were also validated by reverse transcription-quantitative polymerase chain reaction (RT-qPCR) and western blot analysis, respectively. The expression levels of miR-431 were gradually decreased over time periods of E19, E21 and P3, as determined using RT-qPCR and fluorescence *in situ* hybridization. Dual luciferase-reporter assays revealed that SMAD4 is a direct target of miR-431. The mRNA and protein expression levels of SMAD4 and SPs increased gradually in rat lung tissues from E19 to P3. The order of magnitude was as follows: E19, E21 and P3. The present study demonstrated that the expression level of miR-431 decreased in the order of E19, E21 and P3 during rat lung development. The target gene of miR-431, SMAD4, was negatively regulated by miR-431, and its expression levels in the rat lung tissue increased from E19 to the P3.

Surfactant synthesis was further increased over the E19 to P3 time period. Further studies are required to determine how miR-431 regulates pulmonary surfactant synthesis by targeting SMAD4.

Introduction

Advances in perinatal medicine and neonatal intensive care have increased the survival rate of premature infants, and the incidence of respiratory distress syndrome (RDS) and bronchopulmonary dysplasia (BPD). A total of 80,000 cases of RDS have been reported in the United States per year, of which 8,500 cases are cases of neonatal mortality (1). The incidence of BPD is estimated to be 12-32% in preterm infants born at <32 weeks of gestation, and even up to 50% in infants with very low birth weight (<1,000 g) and preterm infants with gestational age <28 weeks (2,3). At lower gestational ages, the lungs are less developed, and incidence of RDS and BPD is higher (4). Although RDS, BPD and other neonatal pulmonary diseases have been studied extensively, these studies have primarily focused on the pathogenesis, progression and prognoses of the diseases examined. A limited number of studies have been associated with the common physiological basis of immature pulmonary development. Thus, investigating of the potential mechanism underlying lung development is imperative to provide important insights for the prevention and control of lung developmental diseases.

MicroRNAs (miRNAs/miRs) are a group of noncoding RNAs (typically 21-24 nucleotides) that have an important role in regulating the expression of target genes at the post-transcriptional level (5,6). miRNA functions have been recently identified to be associated with cell development, cell proliferation, signal transduction, stem cell differentiation and tumor progression (7). To date, a limited number of studies have reported whether miRNAs are involved in lung development. Bhaskaran *et al* (8) reported that overexpression of miR-127 in fetal lung organ culture significantly decreased the terminal bud count, while increasing terminal and internal bud sizes, and causing unevenness in bud sizes, which suggested improper development. Carraro *et al* (9) reported that miR-142-3p balances proliferation and differentiation of mesenchymal cells during lung development. miR-124 levels were also

Correspondence to: Dr Yang Yang, Department of Neonates, Children's Hospital of Nanjing Medical University, 72 Guangzhou Road, Nanjing, Jiangsu 210008, P.R. China
E-mail: yy860507@126.com

Dr Zhi-Dan Bao, Department of Neonates, Jiangyin People's Hospital of Nanjing Medical University, 163 Shoushan Road, Wuxi, Jiangsu 210008, P.R. China
E-mail: 1287755051@qq.com

Key words: microRNA-431, lung development, SMAD4, transforming growth factor- β pathway, surfactant proteins

reported to be downregulated during the later stages of fetal lung development and these alterations could inhibit fetal lung epithelial maturation (10). Despite these promising findings, knowledge is limited regarding the regulation of miRNA expression and their potential role in lung pathophysiology. In our previous study, an miRNA microarray was used to compare the expression levels of miRNAs in venous blood between infants with RDS and infants without RDS. miR-431 was differentially expressed between the two groups, which indicated that it may be associated with occurrence of RDS (11). In addition, we revealed that the expression levels of miR-431 were downregulated gradually following rat lung tissue development as demonstrated by miRNA microarrays (12). Taken collectively, it was hypothesized that miR-431 has an important role in lung tissue development.

In the present study, bioinformatic analysis was performed and demonstrated that SMAD4 (also termed drosophila mothers against decapentaplegic protein 4) is one of the target genes of miR-431. The transforming growth factor- β (TGF- β)/SMAD pathway has been characterized as an important signaling axis that regulates lung development (13). In addition, SMAD4 is an important transcription factor required for the regulation of the TGF- β pathway throughout lung tissue development (14).

Lung tissue development is a continuous and gradual process. The development of the lung tissues in Sprague-Dawley rats can be divided into the following five stages: embryonic stage (E0-E13), the glandular stage (E13-E18), the canalicular stage (E18-E20), the saccular stage (E20 to full term) and the alveolar stage (after birth) (15,16). It is important to note that the onset of surfactant synthesis and microvascular development in the early saccular stage is necessary for lung function at birth. The lack of surfactant proteins (SPs) leads to RDS, and it is also considered a risk factor of BPD (16,17). Among these stages, E19, E21 and P3 time points representing the canalicular, the sacular and the alveolar phases of lung development, respectively, were selected, and the expression and potential regulation of miR-431 in rat lung development by targeting SMAD4 was explored at each stage.

Materials and methods

Rats. The animal procedures in this study were approved by the Nanjing Medical University Animal Care and Use Committee (Nanjing, China). Healthy adult Sprague-Dawley rats (9 female and 9 male; age, 2 months; weight, 350-450 g) were purchased from The Experimental Animal Center of Nanjing Medical University. Animals were housed in a specific pathogen-free animal environment with the temperature between 18-23°C and humidity between 60-65%. Rats had access to food and water *ad libitum*. Whole lungs were isolated from nine rat fetuses on gestational days 19 and 21 (E19 and E21) and from nine 3-day-old rats (weight, 9.361±0.742 g; postnatal day 3; P3). The three time points represent the key three stages of mammalian lung development [the canalicular stage (E18-E20), the sacular stage (E20 to full term), and the alveolar stage], and were designated as groups S1 (E19), S2 (E21) and S3 (P3). For timed pregnancy, the day on which vaginal plugs were discovered was denoted as gestational day 1. For to obtain fetal lungs, pregnant Sprague-Dawley rats were sacrificed using CO₂.

Fetuses were removed from the uterus, and the lungs were isolated from these fetuses without the surrounding tissues. For pup lungs, male Sprague-Dawley rats were sacrificed by cervical dislocation before isolation of the lungs. The left lungs were used for light microscopy observation, miRNA and mRNA detection, while the right lungs were used for electron microscopy observation, fluorescence *in situ* hybridization (FISH) and western blot analysis.

Light microscopy. After isolation, a randomly selected fetal lung was retained for histological observation. Left lung tissue specimens were fixed in formalin at 37°C for 24 h, dehydrated and embedded in paraffin. Continuous sections (thickness, 3 μ m) were stained with hematoxylin and eosin for 10 min at room temperature for subsequent morphological observation. Morphological changes were evaluated using an optical microscope (x20 or x40 magnification; DM2500; Leica Microsystems GmbH, Wetzlar, Germany). Three sections from each mouse were analyzed. In total, ten fields from each section were randomly selected for analysis.

Electron microscopy. The lobe of right lung was cut and divided into several sections, with the size of 0.1x0.1x0.1 cm, then fixed in 2.5% glutaraldehyde at 4°C for 4 h, dehydrated, embedded in epoxy resin, and cut into ultrathin sections (thickness of sections, 50-80 nm) for analysis of the changes of organelles by transmission electron microscopy (JEM-1010; Jeol, Ltd., Tokyo, Japan).

FISH. FISH was performed using 5' fluorescein amidite (FAM)-labeled probes (TsingKe Biological Technology, Beijing, China) for miRNA-431. The lung tissue specimens were fixed in 4% paraformaldehyde (prepared from diethyl pyrocarbonate) for 1-2 h at 37°C. Fixed specimens were dehydrated in 15% sucrose solution for 8 h and in 30% sucrose solution overnight at room temperature. Samples were frozen at -30°C and cut into 4- μ m-thick slides, then dried at room temperature. The slides were again fixed in 4% paraformaldehyde at 37°C for 10 min, and rinsed in PBS (pH 7.4) three times in rocking device for decoloring, for 5 min each time. According to the characteristics of rat lung tissue and index, the slides were digested in proteinase K (20 μ g/ml; cat. no. G1205; Servicebio Inc., Wuhan, China) for 8 min at 37°C, and then washed in PBS three times for 15 min. The slides were pre-hybridized in hybridization buffer (Abnova, Taipei, Taiwan) for 1 h at 37°C in a humidified chamber. The pre-hybridization buffer was removed and the FAM-labeled probes for rno-mir-431 was added at a concentration of 8 ng/ μ l and incubated overnight at the hybridization temperature (37°C). The slides were rinsed in 2X saline-sodium citrate (SSC) for 10 min, 1X SSC twice for 10 min, and washed 0.5X SSC for 10 min, 2X SSC and 1X SSC solution at the same hybridization temperature. The slides were stained with DAPI (cat. no. G1012; Servicebio Inc.) and incubated for 8 min at 4°C, avoiding the light. The anti-fluorescence quenching reagent (cat. no. G1401; Servicebio Inc.) was dripped on after washing. The slides were then mounted, coverslipped, and observed using a Nikon DS-U3 fluorescence microscope (magnification, x40; Nikon Corporation, Tokyo, Japan). The sequence of the rno-miR-431 probe for FISH was 5'-GCATGACGGCCTGCAAGACA-3'.

Table I. Primer sequences for reverse transcription-quantitative polymerase chain reaction.

Gene	Primer sequence
MicroRNA-431	F: 5'-AGGTGTCTTGCAGGCCGT-3' R: 5'-GTGCGTGTTCGTGGAGTCG-3'
U6	F: 5'-GCTTCGGCAGCACATATACTAAAAT-3' R: 5'-CGCTTCACGAATTTGCGTGTTCAT-3'
SMAD4	F: 5'-ATCACTATGAGCGGGTTGT-3' R: 5'-TTGGTGGATGTTGGATGG-3'
SP-A	F: 5'-AGAACGTGGAGACAAGGG-3' R: 5'-TGATCTCATAGAGTTCAGTCTGG-3'
SP-B	F: 5'-AGCCTGGAGCAAGCGATAC-3' R: 5'-AAGCGTCTTCCTTGGTCATC-3'
SP-C	F: 5'-CCTTGTCGTCGTGGTGAT-3' R: 5'-AGGTAGCGATGGTGTCTGT-3'
SP-D	F: 5-GGAATCAAAGGCGAAAGTGG-3' R: 5'-TGCTGTGGGCTGTGACGAG-3'
β -actin	F: 5'-CGAGTACAACCTTCTTGCAGC-3' R: 5'-ACCCATACCCACCATCACAC-3'

SP, surfactant protein; F, forward; R, reverse.

The probe was labeled with fluorescein amidite (Biosearch Technologies, Petaluma, CA, USA).

Target genes prediction and bioinformatics analysis. MiRBase sequence database (<http://www.mirbase.org/>) was used to identify the nucleotide sequence for different species. The target genes of miR-431 were predicted using TargetScan database (www.targetscan.org). The results indicated SMAD4 was a potential target of miR-431.

RNA extraction and reverse transcription-quantitative polymerase chain reaction (RT-qPCR). Total RNA from lung tissue was extracted with TRIzol reagent (Invitrogen; Thermo Fisher Scientific, Inc., Waltham, MA, USA) according to manufacturer instructions. For miR-431 quantification in rat lungs, cDNA was prepared in an RT reaction using the PrimeScript™ RT Reagent kit (Takara Bio, Inc., Otsu, Japan). The reactions were incubated at 16°C for 30 min, 42°C for 40 min and at 85°C for 5 min. RT-qPCR was performed using an Applied Biosystems 7500 Fast real-time PCR cycler (Applied Biosystems; Thermo Fisher Scientific, Inc., Waltham, MA, USA). U6 small nuclear 6 was used as an internal control. The primers (Table I) for miR-431-5p and U6 were designed and purchased from Kangchen Biotech Co., Ltd (Wuhan, China). Amplification was performed with the SYBR® Premix Ex Taq™ (Takara Bio, Inc.) according to the manufacturer's protocol. Thermocycling conditions included an initial step at 95°C for 5 min, and 40 cycles at 90°C for 15 sec, 60°C for 15 sec and 72°C for 1 min, and final extension at 72°C for 10 min.

For mRNA quantification, cDNA was synthesized using PrimeScript™ RT Master Mix (Takara Bio, Inc.). The reactions were incubated at 37°C for 15 min and at 85°C for 5 sec. Expression of SMAD4 and SPs was determined by RT-qPCR

using the SYBR-Green PCR Master Mix (cat. no. RR036A; Takara Bio, Inc.) with the mouse primers. GAPDH primers were used for normalization. All primers (Table I) were designed and purchased from Kangchen Biotech Co., Ltd. Thermocycling conditions included an initial step at 95°C for 30 sec, and 40 cycles at 95°C for 5 sec and 60°C for 34 sec, and final extension at 72°C for 10 min. The relative gene expression was calculated using the $2^{-\Delta\Delta C_q}$ method (18).

Dual luciferase-reporter assay. The wild-type (WT) and mutated (MUT) 3' untranslated region (3'-UTR) sequences of SMAD4 (Guangzhou RiboBio Co., Ltd., Guangzhou, China), which were predicted to have an interaction with miR-431, were inserted into firefly luciferase expressing pmiR-RB-REPORT™ vector (Guangzhou RiboBio Co., Ltd.) in accordance with the manufacturer's protocol. The primer sequences of hsa-SMAD4-3'UTR were the following: forward GCGGCTCGAGACAAGGTTGGTTGCTAAGA and reverse AATGCGGCCGCGGCTGTTGCCTGTCATTTA. Genomic DNA was extracted from 293T cells (Guangzhou RiboBio Co., Ltd.) using the TIANamp Genomic DNA kit (Tiangen Biotech Co., Ltd., Beijing, China). The thermocycling conditions of the PCR were as follows: initial denaturation at 98°C for 2 min, followed by 10 cycles of 98°C for 10 sec, 65°C for 15 sec and 72°C for 45 sec, followed by 15 cycles of 98°C for 10 sec, 60°C for 15 sec and 72°C for 45 sec, with a final extension at 72°C for 3 min. For the luciferase reporter assay, 293T cells were seeded into 96-well plates (1.5×10^4 cells/well). Following culturing for 24 h, cells were co-transfected with the indicated vectors (250 ng/well), 50 nM miR-431 mimics (cat. no. miR10001625; Guangzhou RiboBio Co., Ltd.) or miR-431 mimic negative control (NC) (cat. no. miR1N0000001-1-5; Guangzhou RiboBio Co., Ltd.) using 250 ng/well Lipofectamine® 3000 (Invitrogen; Thermo Fisher Scientific, Inc.). At 48 h post-transfection,

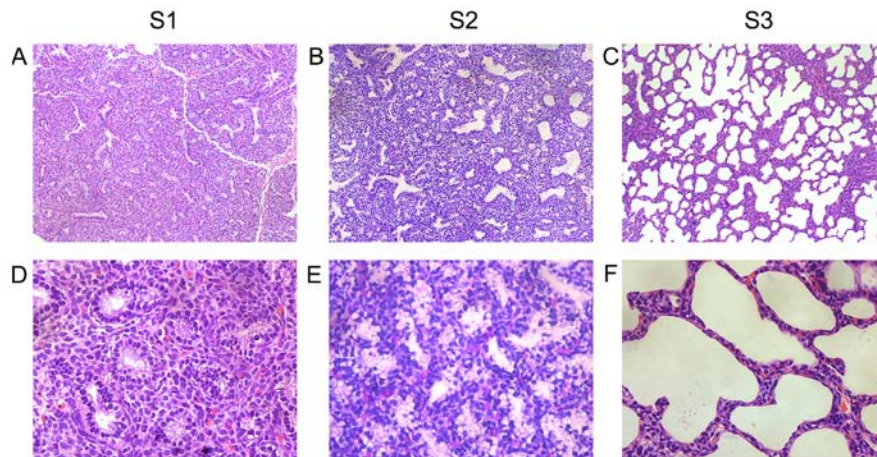


Figure 1. Hematoxylin and eosin staining of rat lung tissue at the three stages under an optical microscope, H&E. (A-C) x20 objective. (D-F) x40 objective. S1, embryonic day 19; S2, embryonic day 21; S3, postnatal day 3.

the cells were lysed and luciferase activity was assayed using the Dual-Luciferase Reporter Assay system (Promega Corporation, Madison, WI, USA). The Firefly luciferase activity was evaluated after normalization to Renilla activity.

Western blot analysis. The following antibodies were used as primary antibodies for western blot analysis: monoclonal rabbit anti-mouse SMAD4 antibody (1:2,000; cat. no. ab40759; Abcam), polyclonal rabbit anti-mouse SP-A antibody (1:500; cat. no. SAB4300719; Sigma-Aldrich; Merck KGaA, Darmstadt, Germany), polyclonal rabbit anti-mouse SP-B antibody (1:1,000; cat. no. NBP1-57977; Novus Biologicals, LLC, Littleton, CO, USA), monoclonal mouse anti-mouse SP-C antibody (1:1,000; cat. no. MA5-17172; Invitrogen; Thermo Fisher Scientific, Inc.), monoclonal rabbit anti-mouse SP-D antibody (1:1,000; cat. no. ab168366; Abcam), or monoclonal rabbit anti-mouse β -actin antibody (1:2,000; cat. no. 4970; Cell Signaling Technology, Inc., Danvers, MA, USA).

The isolated lung specimens were washed three times with PBS, and then lysed with phenylmethylsulfonyl fluoride (1 mM; cat. no. G2008; Servicebio Inc.). Total protein was extracted from these specimens and then quantified using a bicinchoninic acid protein assay kit (cat. no. G2026; Servicebio Inc.). A total of 50 μ g protein was loaded in each well. Proteins were separated by 10% SDS-PAGE. Electrotransfer onto PVDF membranes was performed for 1.5 h on ice. The membranes were blocked for 1 h at room temperature in 5% non-fat dry milk in TBS+0.05% Tween-20 (TBST), followed by incubation at 4°C overnight with primary antibodies. After washing with TBST three times, the membranes were incubated with horseradish peroxidase (HRP)-conjugated goat anti-mouse secondary antibody (1:3,000; cat. no. GB23303; Servicebio Inc.) or HRP-conjugated goat anti-rabbit secondary antibody (1:3,000; cat. no. GB23302; Servicebio Inc.) at 37°C for 1 h, followed by a further three washes with TBST. The protein expression levels were normalized to that of β -actin on the same membrane to confirm equal loading. The protein signals were detected using an enhanced chemiluminescence kit (cat. no. G2014; Servicebio Inc.) and analyzed with ImageJ software (version 2.1; National Institutes Health).

Statistical analysis. Data were analyzed using the SPSS 19.0 software (IBM Corp., Armonk, NY, USA). Values are presented the mean \pm standard deviation. One-way analysis of variance followed by Tukey's test was applied to analyze statistical significance among three groups, while Student's t-test was used to compare two groups. All experiments were repeated independently at least three times. $P < 0.05$ was considered to indicate a statistically significant difference.

Results

Light microscopy. In group S1 (E19), bronchioles were evident. The interstitium was thick and primal alveolar cells surrounded by monolayer cubic epithelial cells were visible (Fig. 1A and D). In group S2 (E21), the number of alveoli increased and the alveolar structures expanded. The stromal layer developed and became thinner than that noted earlier. The cuboidal epithelial cells were gradually flattened (Fig. 1B and E). In group S3 (P3), the shaping of the secondary septum was initiated. The stromal layer was thinner than that noted in the earlier groups and alveolar cavities were considerably expanded (Fig. 1C and F).

Electron microscopy. Type II alveolar epithelial differentiation was observed in group S1 (E19). A limited number of microvilli were present on the free surface of the cells. Osmiophilic multilamellar bodies appeared for the first time in the cytoplasm, which were polycentric or parallel lamellar structures with deep staining (Fig. 2A). In group S2 (E21), type II alveolar epithelial cells were enlarged. The number of short microvilli on the cell surface and lamellar bodies increased. A higher number of mitochondria and multivesicular bodies were simultaneously observed in the cytoplasm (Fig. 2B). In group S3 (P3), the lamellar structure became more dense. The number of lamellar bodies was increased and tended to aggregate in the cytoplasm (Fig. 2C).

Expression levels of miR-431 during rat lung development. The expression levels of miR-431 were measured by RT-qPCR during the three different stages of the rat lung tissue development, namely gestational days 19 and 21 (E19,

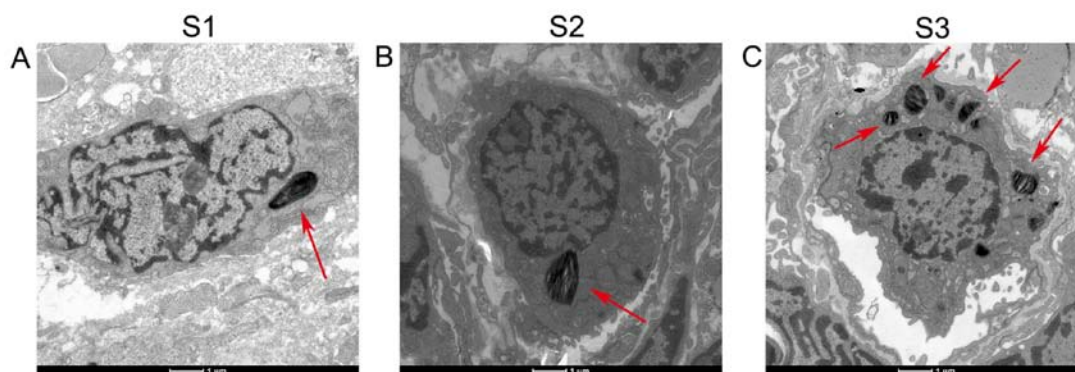


Figure 2. Electro microscopy images of rat lung tissue at three, x4,800 magnification. Red arrows in the picture indicate lamellar bodies. (A) Type II alveolar cells with microvilli and lamellar bodies appeared. (B) The lamellar bodies became larger and the layer structure became clearer than S1. (C) The number of lamellar bodies increased and tended to aggregate. S1, embryonic day 19; S2, embryonic day 21; S3, postnatal day 3.

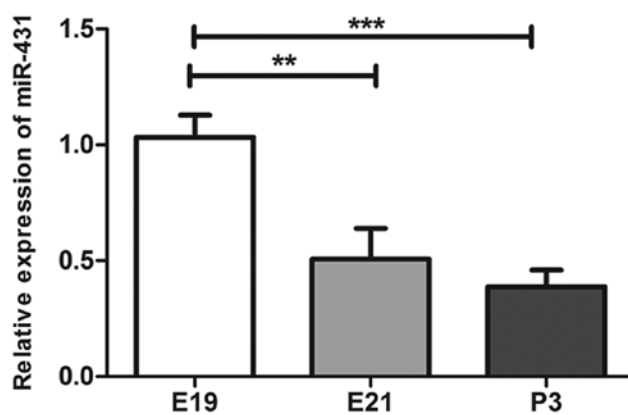


Figure 3. miR-431 expression at the three stages during rat lung development determined by reverse transcription-quantitative PCR. ** $P < 0.01$, *** $P < 0.001$. miR-431, microRNA-431; E19, embryonic day 19; E21, embryonic day 21; P3, postnatal day 3.

E21), and postnatal day 3 (P3; Fig. 3). The three time points represent the key three stages of mammal lung development [the canalicular stage (E18-E20), the saccular stage (E20 to full term), and the alveolar stage]. The expression levels of miR-431 were significantly decreased at E21 compared with E19 ($P < 0.05$) and were continuously decreased at P3 compared with E21. FISH analysis of miR-431 expression is shown in Fig. 4. miR-431 was localized in the cytoplasm and exhibited higher signal intensity at E19. The fluorescence intensity was gradually decreased from E19 to P3 (Fig. 4).

SMAD4 was identified as a target of miR-431. Target prediction was performed using TargetScan to identify the potential target of miR-431. As shown in Fig. 5A, SMAD4 contained the putative binding sites for miR-431 and was predicted as one of the target genes. The sequence 'GCAAGAC' of the SMAD4 3'-UTR that matches 'CGUUCUG' in miR-431 is highly conserved among species (Fig. 5C). In order to validate the accuracy of the prediction, a dual luciferase reporter assay was performed. Upregulation of miR-431 significantly down-regulated the luciferase activity of the SMAD4-WT 3'-UTR ($P < 0.01$; Fig. 5B). These results indicated that miR-431 directly targeted SMAD4-WT. In addition, there was a significant increase in the luciferase activity of 293T cells transfected

with a mutant SMAD4 3'UTR (SMAD4-mut) in the miR-431 mimics compared with the NC groups ($P < 0.001$).

Expression levels of SMAD4 and SPs during rat lung development. In order to explore the effects of miRNA-431 on SMAD4 and the synthesis and secretion of the surfactants during rat lung development, rat lung tissues were isolated during three development stages and measured the expression levels of SMAD4, SP-A, SP-B, SP-C and SP-D. The expression levels of miR-431 were downregulated from E19 to P3, whereas the mRNA levels of SMAD4, SP-A, SP-B, SP-C and SP-D were increased gradually, as determined by RT-qPCR (Fig. 6). These changes were statistically significant (Fig. 6). In addition western blot analysis was performed to determine the expression of SMAD4 and SPs at the protein level. Similar statistically significant trends were noted for SMAD4 and SP markers with regard to the expression of their mRNA and protein levels (Fig. 7).

Discussion

miR-431 is an oncogenic miRNA associated with the initiation and development of human cancer. Currently, certain studies have provided new insight regarding the biological functions of miR-431. Han *et al* (19) reported that miR-431 had protective effects against cerebral ischemia-reperfusion injury in rats by targeting the Rho/Rho-kinase signaling pathway. Wu and Murashov (20) demonstrated that miR-431 regulated axon regeneration in mature sensory neurons. An additional study has shown that miR-431 regulates differentiation and regeneration of old skeletal muscle (21). The common findings of these studies indicate that miR-431 is associated with organ maturation. In the present study, we hypothesized miR-431 is associated with the regulation of lung tissue development. RT-qPCR and FISH analyses demonstrated that the expression levels of miR-431 were decreased from E19 to P3. In a previous study, our group used miRNA microarray analysis to compare the expression levels of miR-431, and found higher expression levels of this miRNA in patients with RDS than in infants without RDS (11). Therefore, miR-431 may have a negative impact on the regulation on lung development.

Lung development extends from the embryonic period to the fetal period, up to birth and afterwards (22). During the

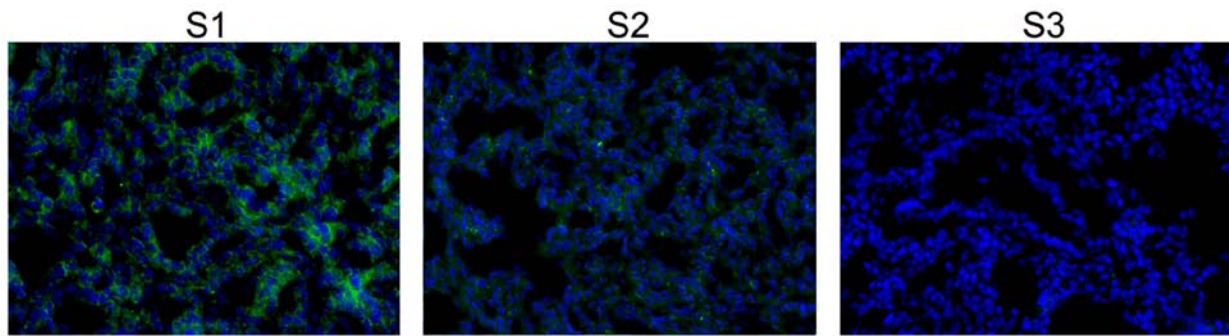


Figure 4. miR-431 expression in three stages of rat lung development determined by fluorescence *in situ* hybridization. Green fluorescence signal indicated miR-431 expression. Strong signal in S1, weaker in S2 and almost no green signal in S3. miR-431, microRNA-431; S1, embryonic day 19; S2, embryonic day 21; S3, postnatal day 3.

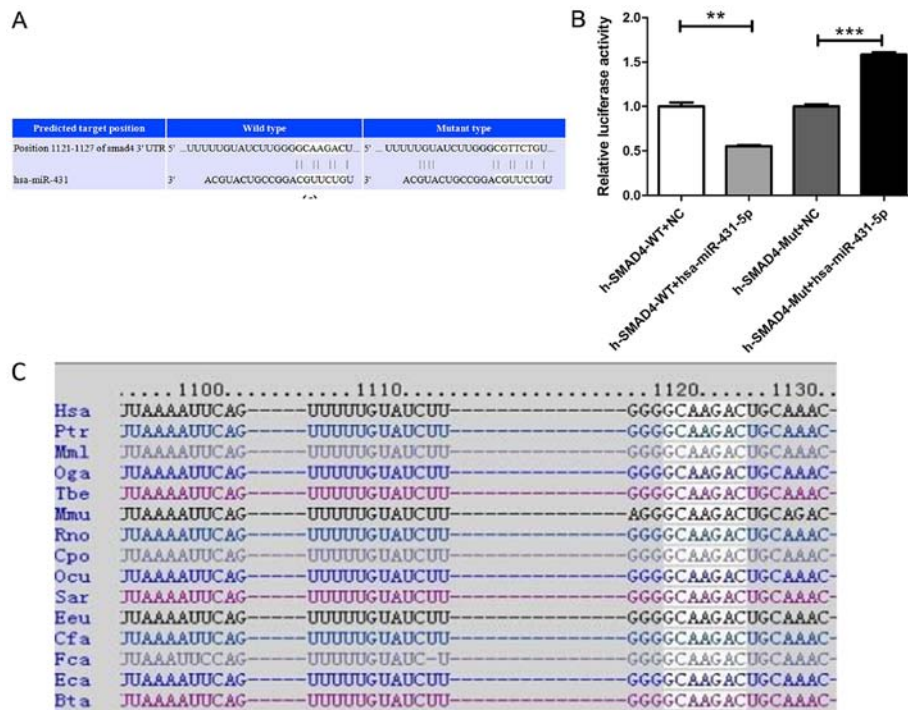


Figure 5. SMAD4 is a target of miR-431-5p. (A) TargetScan predicted position 1,121-1,127 of the SMAD4 3'-UTR as a binding site for miR-431. (B) Luciferase activity of SMAD4 3'-UTR-WT and SMAD4 3'-UTR-MUT in the presence of miR-431-5p mimic or NC. (C) GCAAGAC is a highly conserved sequence of Smad4, and it is present in different species, as predicted by TargetScan database. ** $P < 0.01$, *** $P < 0.001$. 3'-UTR, 3' untranslated region; miR-431-5p, microRNA-431-5p; WT, wild-type; NC, negative control; MUT, mutant.

pseudoglandular stage, the epithelial tube undergoes branching morphogenesis so that the conduction part of the respiratory system reaches to the level of distal bronchioles. At this stage the bronchial tree and parts of the parenchyma are formed. During the canalicular stage of lung development, distal airway bronchioles begin to shape and this process is accompanied by proximal to distal epithelial differentiation. One of the main features of this stage is the onset of the air-blood barrier. In the saccular stage of lung development, the formation of terminal saccules was gradually formed, and the epithelial cell differentiation into secretory rounded type II and squamous type I pneumocytes was initiated. Airspaces expand and the surfactant forms. During the alveolar stage (last stage of lung development), alveolarization aims to increase the gas exchange surface area. In humans, the alveolar stage is initiated during the late fetal period and continues into childhood.

In rodents, alveolarization is predominantly postnatal (15). In the present study, it was observed that lamellar bodies, which are intracellular storage units of pulmonary surfactant, were present in alveolar cells on E19. Following lung development, the number of lamellar bodies was gradually increased, and the staining was enhanced, which suggested enhanced function. From E19 to P3, the stromal layer became thinner and capillary networks were gradually generated.

Several signaling pathways are associated with lung tissue development, such as the TGF- β , bone morphogenetic proteins and Wnt pathways (23-25). Notably, TGF- β exerts a key role in normal lung morphogenesis and function (26,27). Previous studies have demonstrated that TGF- β is expressed at high levels during normal lung development and that the expression levels of TGF- β determine branching morphogenesis and epithelial cell differentiation with maturation

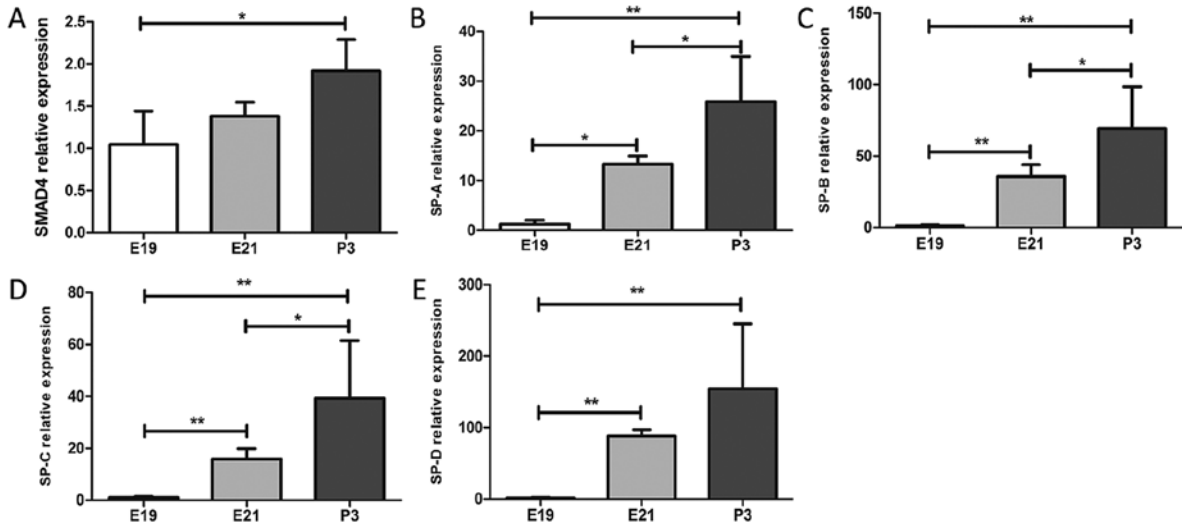


Figure 6. Reverse transcription-quantitative PCR was used to detect the expression of SMAD4 and SPs. The expressions of (A) SMAD4 mRNA, (B) SP-A mRNA, (C) SP-B mRNA, (D) SP-C mRNA and (E) SP-D mRNA were upregulated from E19 to P3. * $P < 0.05$, ** $P < 0.01$. E19, embryonic day 19; E21, embryonic day 21; P3, postnatal day 3; SP, surfactant protein.

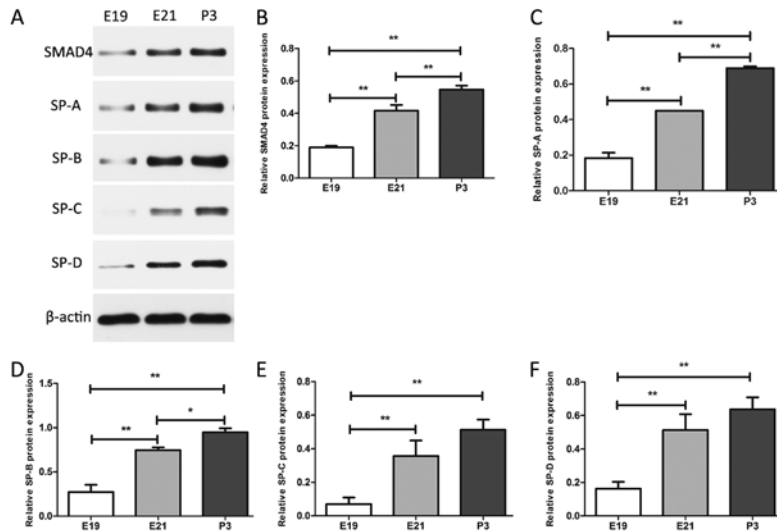


Figure 7. Western blot analysis of the protein expression of SMAD4 and SPs. (A) Western blot analysis and densitometry of (B) SMAD4, (C) SP-A, (D) SP-B, (E) SP-C and (F) SP-D protein at three stages. * $P < 0.05$, ** $P < 0.01$. E19, embryonic day 19; E21, embryonic day 21; P3, postnatal day 3; SP, surfactant protein.

of surfactant synthesis (13). The SMAD family of proteins is an important intracellular mediator of TGF- β signaling and can be divided into three functional classes as follows: Receptor-regulated SMAD (R-SMAD), the co-mediator SMAD (Co-SMAD), and the inhibitory SMAD (I-SMAD). R-SMADs (SMAD1, 2, 3, 5 and 8) are directly phosphorylated and activated by the type I receptor kinases and can undergo homotrimerization in order to form heteromeric complexes with Co-SMAD and SMAD4 (28,29). As a key nuclear transcription factor, SMAD4 transfers the signal from the activated receptor to the nucleus to regulate gene expression. It has been demonstrated that miR-27a regulates the TGF- β signaling pathway by targeting SMAD4 in lung cancer (30). Cui *et al* (31) indicated that miR-27a-3p acted as a negative regulator of lung fibrosis by directly targeting SMAD2 and SMAD4. In the present study, bioinformatic analysis suggested that SMAD4 is a potential target gene

of miR-431. The sequence of SMAD4 3'-UTR binding with miR-431 is highly conserved among species. A dual luciferase reporter assay was performed to demonstrate that miR-431 directly targets SMAD4-WT. Notably, there was a statistical difference in luciferase activity when comparing the Smad4-WT+miR-431-5p group and the Smad4-WT+NC group. Interestingly, the luciferase activity in the Smad4-MUT+miR-431-5p group increased significantly compared with the Smad4-MUT+NC group. This may be due to the fact that miRNAs have pleiotropic roles, and the expression of target genes is influenced by various unknown factors. The dual luciferase-reporter assay actually reflected the interaction of miRNA-431 with various potential molecules in cells. Therefore, the increase in luciferase activity in the Smad4-MUT+miR-431-5p group may be influenced by multiple factors, which require further investigation. The expression levels of SMAD4 were subsequently compared

among the three development stages. The expression levels of SMAD4 were increased with the increasing age of the rats (E19, E21, P3), which was the opposite of the trend noted for miR-431. Taken collectively, the data suggested that miR-431 negatively regulates SMAD4 expression.

Pulmonary surfactant is a complex with a unique phospholipid and protein composition. Its specific function is to reduce surface tension at the pulmonary air-liquid interface (32). Lack of pulmonary surfactant due to lung immaturity can lead to RDS. To date, four types of SPs (SP-A, SP-B, SP-C and SP-D) have been identified. It was previously reported that overexpression of miR-124 inhibited the mRNA expression levels of SP-A, SP-B and SP-C (10). Another previous study demonstrated that overexpression of miR-26a in alveolar epithelial type II cells inhibited the synthesis of SP-B and SP-C (33). In the present study, the expression levels of SP mRNA and protein were increased with lung development (from E19 to P3), which was contradictory to the trend noted for miR-431 expression. However, the precise association between miR-431 and SP protein expression requires further investigation.

In conclusion, the current study demonstrated that the expression levels of miR-431 were decreased from E19 to P3 during rat lung development. SMAD4 was identified as a target gene of miR-431 and was negatively regulated by miR-431, with SMAD4 expression levels increased in the rat lung tissue from E19 to P3. Surfactant synthesis was additionally increased from E19 to P3. Whether miR-431 can downregulate pulmonary surfactant synthesis by targeting SMAD4 expression requires further investigation. In summary, these results add provide more insight on the mechanism of lung development and provide a potential direction for the prevention or treatment of RDS, and for the treatment of chronic lung diseases.

Acknowledgements

Not applicable.

Funding

The present study was supported by the National Natural Scientific Grand (grant nos. 81601321, 81741052 and 81871195) from the Government of China, and by the Jiangsu Province Young Medical Talents' Project of 'Science Education Facilitating Health' (grant no. QNRC2016092).

Availability of data and materials

The datasets used and/or analyzed during the current study are available from the corresponding author on reasonable request.

Authors' contributions

ZS, YS and YY contributed to the conception and design of the experiments, the analysis and interpretation of data, and the manuscript preparation and critical evaluation. ZB and XC contributed to the experimental study, the data interpretation and the statistical analysis and manuscript preparation. XZ and RC contributed to the experimental study conduct, the data

interpretation and the statistical analysis. All authors reviewed the manuscript.

Ethics approval and consent to participate

All experimental protocols were conducted with the approval of the Nanjing Medical University Animal Care and Use Committee (Nanjing, China).

Patient consent for publication

Not applicable.

Competing interests

The authors declare that they have no competing interests.

References

1. Edwards MO, Kotecha SJ and Kotecha S: Respiratory distress of the term newborn infant. *Paediatr Respir Rev* 14: 29-36, quiz 36-37, 2013.
2. Jensen EA and Schmidt B: Epidemiology of bronchopulmonary dysplasia. *Birth Defects Res A Clin Mol Teratol* 100: 145-157, 2014.
3. Strueby L and Thébaud B: Advances in bronchopulmonary dysplasia. *Expert Rev Respir Med* 8: 327-338, 2014.
4. Stoll BJ, Hansen NI, Bell EF, Shankaran S, Laptook AR, Walsh MC, Hale EC, Newman NS, Schibler K, Carlo WA, *et al*; Eunice Kennedy Shriver National Institute of Child Health and Human Development Neonatal Research Network: Neonatal outcomes of extremely preterm infants from the NICHD Neonatal Research Network. *Pediatrics* 126: 443-456, 2010.
5. Bartel DP: MicroRNAs: Genomics, biogenesis, mechanism, and function. *Cell* 116: 281-297, 2004.
6. Yates LA, Norbury CJ and Gilbert RJ: The long and short of microRNA. *Cell* 153: 516-519, 2013.
7. Ambros V: The functions of animal microRNAs. *Nature* 431: 350-355, 2004.
8. Bhaskaran M, Wang Y, Zhang H, Weng T, Baviskar P, Guo Y, Gou D and Liu L: MicroRNA-127 modulates fetal lung development. *Physiol Genomics* 37: 268-278, 2009.
9. Carraro G, Shrestha A, Rostkovicus J, Contreras A, Chao CM, El Agha E, Mackenzie B, Dilai S, Guidolin D, Taketo MM, *et al*: miR-142-3p balances proliferation and differentiation of mesenchymal cells during lung development. *Development* 141: 1272-1281, 2014.
10. Wang Y, Huang C, Chintagari NR, Xi D, Weng T and Liu L: miR-124 regulates fetal pulmonary epithelial cell maturation. *Am J Physiol Lung Cell Mol Physiol* 309: L400-L413, 2015.
11. Kan Q, Ding S, Yang Y and Zhou X: Expression profile of plasma microRNAs in premature infants with respiratory distress syndrome. *Mol Med Rep* 12: 2858-2864, 2015.
12. Yang Y, Kai G, Pu XD, Qing K, Guo XR and Zhou XY: Expression profile of microRNAs in fetal lung development of Sprague-Dawley rats. *Int J Mol Med* 29: 393-402, 2012.
13. Bartram U and Speer CP: The role of transforming growth factor β in lung development and disease. *Chest* 125: 754-765, 2004.
14. ten Dijke P and Hill CS: New insights into TGF- β -Smad signalling. *Trends Biochem Sci* 29: 265-273, 2004.
15. Zoetis T and Hurtt ME: Species comparison of lung development. *Birth Defects Res B Dev Reprod Toxicol* 68: 121-124, 2003.
16. Burri PH: Fetal and postnatal development of the lung. *Annu Rev Physiol* 46: 617-628, 1984.
17. Bernhard W: Lung surfactant: function and composition in the context of development and respiratory physiology. *Ann Anat* 208: 146-150, 2016.
18. Livak KJ and Schmittgen TD: Analysis of relative gene expression data using real-time quantitative PCR and the 2(-Delta Delta C(T)) Method. *Methods* 25: 402-408, 2001.
19. Han XR, Wen X, Wang YJ, Wang S, Shen M, Zhang ZF, Fan SH, Shan Q, Wang L, Li MQ, *et al*: Protective effects of microRNA-431 against cerebral ischemia-reperfusion injury in rats by targeting the Rho/Rho-kinase signaling pathway. *J Cell Physiol* 233: 5895-5907, 2018.

20. Wu D and Murashov AK: MicroRNA-431 regulates axon regeneration in mature sensory neurons by targeting the Wnt antagonist Kremen1. *Front Mol Neurosci* 6: 35-48, 2013.
21. Lee KP, Shin YJ, Panda AC, Abdelmohsen K, Kim JY, Lee SM, Bahn YJ, Choi JY, Kwon ES, Baek SJ, *et al*: miR-431 promotes differentiation and regeneration of old skeletal muscle by targeting Smad4. *Genes Dev* 29: 1605-1617, 2015.
22. Mullasery D and Smith NP: Lung development. *Semin Pediatr Surg* 24: 152-155, 2015.
23. Hata A and Chen YG: TGF- β Signaling from receptors to smads. *Cold Spring Harb Perspect Biol* 8: a022061, 2016.
24. Shi Y and Massagué J: Mechanisms of TGF- β signaling from cell membrane to the nucleus. *Cell* 113: 685-700, 2003.
25. Weng T and Liu L: The role of pleiotrophin and β -catenin in fetal lung development. *Respir Res* 11: 80-80, 2010.
26. Roth-Kleiner M and Post M: Similarities and dissimilarities of branching and septation during lung development. *Pediatr Pulmonol* 40: 113-134, 2005.
27. Chen XQ, Wu SH, Luo YY, Li BJ, Li SJ, Lu HY, Jin R and Sun ZY: Lipoxin A4 attenuates bronchopulmonary dysplasia via upregulation of Let-7c and downregulation of TGF- β 1 signaling pathway. *Inflammation* 40: 2094-2108, 2017.
28. Verhamme FM, Bracke KR, Joos GF and Brusselle GG: Transforming growth factor- β superfamily in obstructive lung diseases. more suspects than TGF- β alone. *Am J Respir Cell Mol Biol* 52: 653-662, 2015.
29. Mehra A and Wrana JL: TGF-beta and the Smad signal transduction pathway. *Biochem Cell Biol* 80: 605-622, 2002.
30. Chae DK, Ban E, Yoo YS, Kim EE, Baik JH and Song EJ: MIR-27a regulates the TGF- β signaling pathway by targeting SMAD2 and SMAD4 in lung cancer. *Mol Carcinog* 56: 1992-1998, 2017.
31. Cui H, Banerjee S, Xie N, Ge J, Liu R-M, Matalon S, Thannickal VJ and Liu G: MicroRNA-27a-3p is a negative regulator of lung fibrosis by targeting myofibroblast differentiation. *Am J Respir Cell Mol Biol* 54: 843-852, 2016.
32. Whitsett JA and Weaver TE: Hydrophobic surfactant proteins in lung function and disease. *N Engl J Med* 347: 2141-2148, 2002.
33. Zhang XQ, Zhang P, Yang Y, Qiu J, Kan Q, Liang HL, Zhou XY and Zhou XG: Regulation of pulmonary surfactant synthesis in fetal rat type II alveolar epithelial cells by microRNA-26a. *Pediatr Pulmonol* 49: 863-872, 2014.